Magnetic Moment Collapse-Driven Mott Transition in MnO

J. Kuneš*

Theoretical Physics III, Center for Electronic Correlations and Magnetism, Institute of Physics, University of Augsburg, Augsburg 86135, Germany and Institute of Physics, Academy of Sciences of the Czech Republic, Cukrovarnická 10, 162 53 Praha 6, Czech Republic

A. V. Lukoyanov

Ural State Technical University-UPI, 620002 Yekaterinburg, Russia

V. I. Anisimov

Institute of Metal Physics, Russian Academy of Sciences-Ural Division, 620041 Yekaterinburg GSP-170, Russia

R. T. Scalettar and W. E. Pickett

Department of Physics, University of California Davis, Davis, California 95616

(Dated: July 27, 2007)

*Electronic address: jan.kunes@physik.uni-augsburg.de

The metal-insulator transition in correlated electron systems, where electron states transform from itinerant to localized, has been one of the central themes of condensed matter physics for more than half a century. The persistence of this question has been a consequence both of the intricacy of the fundamental issues and the growing recognition of the complexities that arise in real materials, even when strong repulsive interactions play the primary role. The initial concept of Mott was based on the relative importance of kinetic hopping (measured by the bandwidth) and on-site repulsion of electrons. Real materials, however, have many additional degrees of freedom that, as is recently attracting note, give rise to a rich variety of scenarios for a "Mott transition." Here we show that the computational theory of strongly correlated systems has progressed to the point where the Mott transition of the classic correlated insulator MnO can be obtained directly from first principles, and the mechanism identified as collapse of the magnetic moment due to increase of the crystal field splitting, rather than to variation of the bandwidth.

We consider, as one of the simpler examples of the canonical Mott insulators,[1] the rocksalt structure transition metal monoxide (TMMO) manganese oxide with half-filled $3d$ shell. MnO is, most certainly, a multiorbital multielectron system with the accompanying complexities of the tenfold degeneracy, but the half-filled $3d$ states under ambient conditions lead to a spherical spin-only magnetic moment. Applying pressure to such a system leads to a number of changes, including insulator-metal transition, orbital repopulation, moment reduction, and volume collapse if a first-order transition results. These changes may occur simultaneously, or sequentially over a range of volumes.[2] Any of these may be accompanied by a structural phase transition, that is, a change in crystal symmetry, but an isostructural volume collapse may occur as well. The $3d$ bandwidth of such a Mott insulator is very susceptible to applied pressure, and has been thought to be one of the main controlling factors in the transition.

While MnO's half-filled shell seems to give it a connection to well studied models, this aspect also makes it atypical of transition metal monoxides, as shown by Saitoh *et al.* who compiled[3] effective parameters for TMMOs from spectroscopic information. An effective intra-atomic Coulomb repulsion energy U_{eff} as defined by them is roughly twice as large

as for the other $3d$ monoxides, and this has been used to suggest that MnO may be the most strongly correlated TMMO. The complexity that should be expected can be grasped by listing the relevant energy scales: $3d$ bandwidth W, Coulomb repulsion U, intra-atomic $d-d$ exchange energy (Hund's rule) J, crystal field splitting $\Delta_{cf} = \varepsilon_{e_g} - \varepsilon_{t_{2g}}$, and charge transfer energy $\Delta_{ct} \equiv \varepsilon_{t_{2g}} - \varepsilon_p$ [the difference in Mn $3d$ (we use t_{2g}) and O $2p$ site energies]. All of these scales evolve as the volume decreases, altering the various microscopic processes and making the pressure-driven Mott transition a challenging phenomenon to describe.

Early shock data[4], and then Raman and optical studies,[5, 6] had identified a transformation in MnO in the neighborhood of 90-105 GPa. Transport,[7] magnetic,[7] structural and spectroscopic,[8, 9] and reflectivity[5] data all point to a first-order, insulator-metal Mott transition near 100 GPa with (reduced) volume ($v = V/V_\circ$) collapse v=0.68→0.63, and moment collapse (from $\sim 5\mu_B$ to $1\mu_B$ or less[8, 9]). The structural data indicates a B1→B8 change just before the Mott transition, which thus occurs within the B8 (NiAs) phase rather than the B1 (NaCl) phase. Since the local environment of the Mn ion remains the same, this structural change is not expected to have much effect on the Mott transition in the disordered phase.

Our dynamical mean field theory (DMFT) approach moves significantly beyond the methods used earlier for TMMOs, by including a full thermodynamic average of local dynamic processes resulting from the strong interaction. Cohen, Mazin, and Isaak calculated the energy and magnetic moment using only local density approximation (LDA) based interactions.[10] In LDA MnO metalizes at (much too) low pressure; within the metallic phase they obtained a moment and volume collapse around 150 GPa. Fang and collaborators addressed this difficulty by using LDA only for the high pressure phase, and modeling the low pressure phase with the correlated LDA+U method.[11] With two different functionals, however, it is not possible to obtain the transition pressure. Four correlated electronic structure methods [12], applied through the volume range of interest, have probed the behavior of MnO under pressure; all obtained a high spin (HS, $S = \frac{5}{2}$) to low spin (LS, $S = \frac{1}{2}$) moment collapse but their predictions differed considerably in other respects, demonstrating that the specific treatment of correlation effects is crucial. The prediction of the LDA+U method, which is regarded as the static, T=0 limit of the theory we use, is found to be affected by magnetic order,[13] and predicts a zero temperature moment collapse in an insulator-insulator transition around

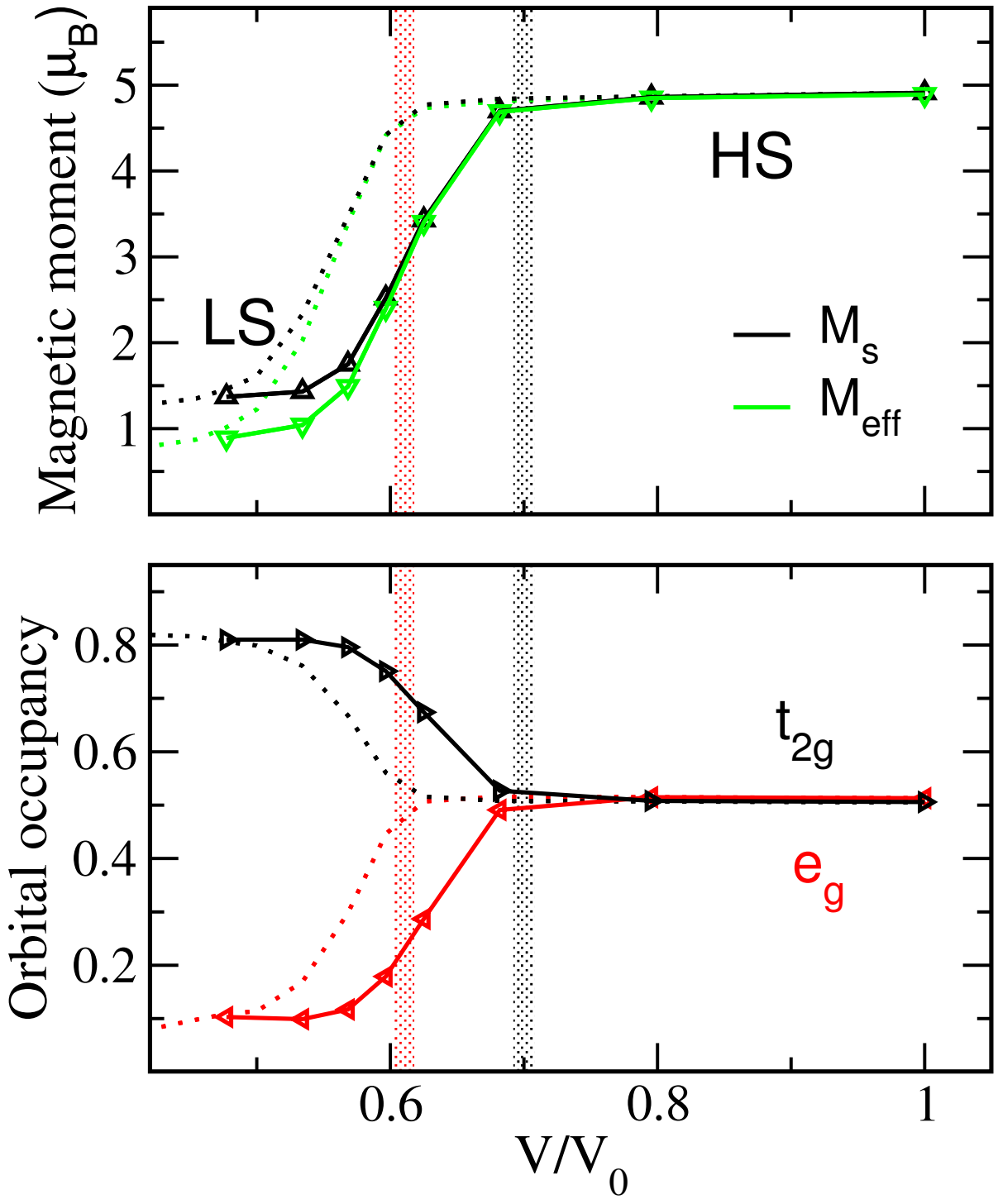

FIG. 1: Evolution of Mn local moment (upper panel) and 3d orbital occupancies (bottom panel) with relative volume. The average instantaneous local moment M_s (black) and effective local moment M_{eff} (green) are compared. The Mn 3d orbital occupancies are resolved into e_g (red) and t_2g (black) components. The solid lines represent the results obtained with U=6.9 eV, J=0.86 eV; the dashed lines using the enhanced value J=1 eV and constant U/J ratio illustrates how the moment collapse is suppressed to smaller volume if the spin-exchange coupling in increased. Closing of the t_{2g} and e_g gaps is indicated by the black and red vertical lines respectively. The analogous closing of the gaps for the dotted line case (J=1 eV) is shifted correspondingly (not shown here).

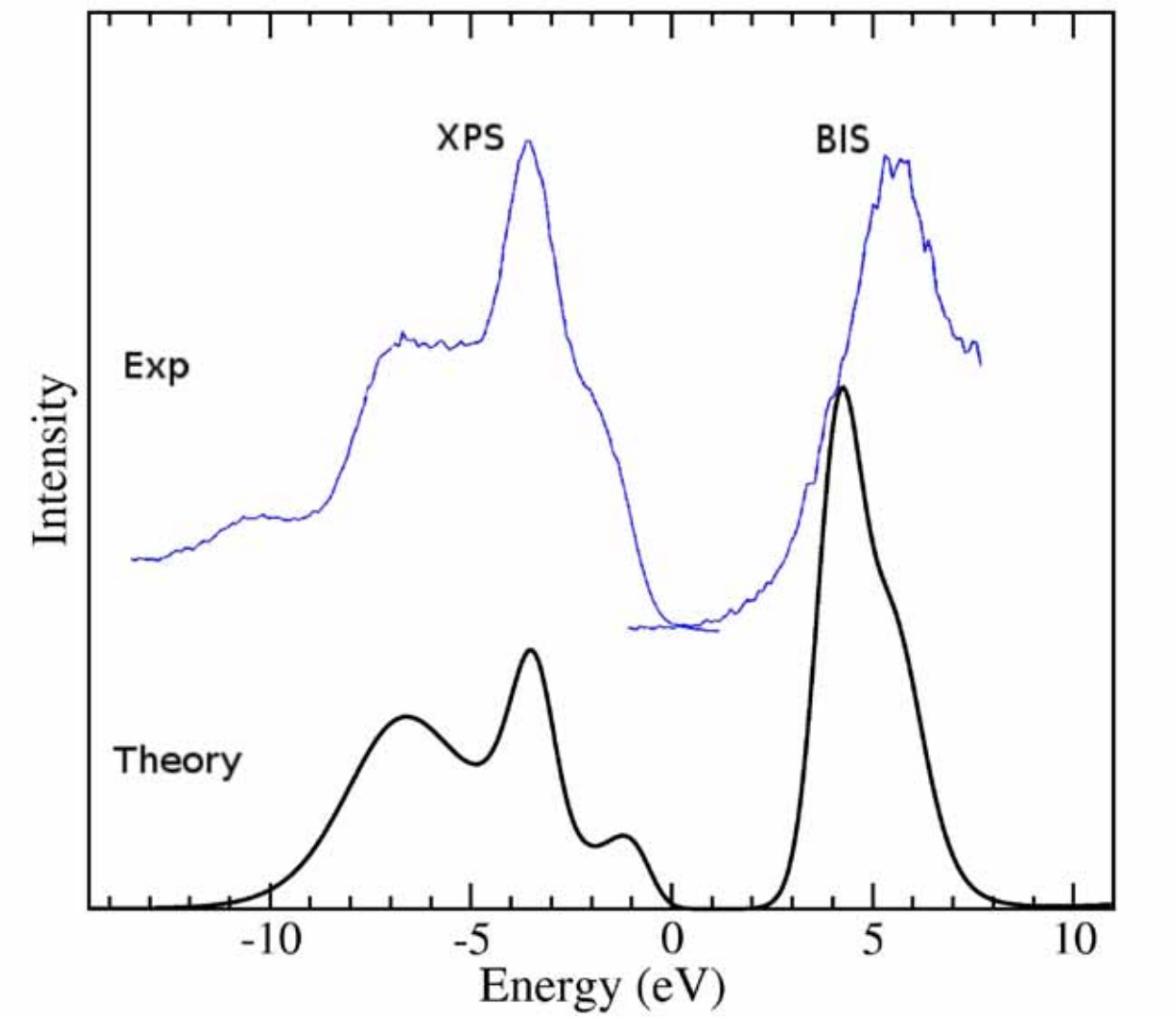

FIG. 2: Ambient pressure x-ray photoemission spectroscopy (XPS) and bremsstrahlung isochromat spectroscopy (BIS) data of van Elp *et al.*[20] on both sides of the energy gap (upper curve offset for clarity) for MnO, compared with the present DMFT result (bottom curve). While the separation of the main peaks is underestimated by $\sim 10\%$, the overall agreement in positions of structure is excellent.

120 GPa (the pressure depends on the value of J), with little difference between the B1 and B8 structure results. Thermodynamic fluctuations have not been included in any previous study.

The LDA+DMFT computational scheme[14] in its present implementation, applied previously to NiO [15], proceeds in two steps: (i) construction of an effective multi-band Hubbard

Hamiltonian via Wannier transformation from a converged (unpolarized, metallic) LDA calculation, and (ii) self-consistent solution of the DMFT equations [16] using the quantum Monte-Carlo impurity solver.[17] The basis set (effectively all-electron) spans the O $2p$ and Mn $3d$ bands plus an additional polarization state with Mn s symmetry. The on-site Coulomb interaction within the Mn $3d$ shell, restricted to density-density terms only, was expressed as usual in terms of the direct (U) and exchange (J) interaction strengths related to the Slater integrals F_0, F_2, F_4. The numerical values of U=6.9 eV and J=0.86 eV[18] were obtained by the constrained LDA method[19]. Since they exhibit only a small pressure dependence, these values were used for all volumes. To obtain an indication of the robustness our results we perform, in parallel with these *ab initio* interaction strengths, calculations with an enhanced (by 15%) value of J=1 eV (and fixed U/J ratio). All the presented results were obtained at the temperature T=1160 K, in the rocksalt structure.

We start the presentation of our results with Fig. 1, showing the evolution of the local magnetic moment and Mn $3d$ occupancies with volume. We use two different measures of the local moment: (a) the mean instantaneous moment defined as an equal time correlation function $M_s = \sqrt{\langle \hat{m}_z^2 \rangle}$ and (b) effective local moment defined through the local spin susceptibility $M_{eff} = \sqrt{T\chi_{loc}}$, which yield similar T-independent values in materials with Curie-Weiss behavior. Under compression, the local moment and Mn $3d$ orbital occupancies retain their ambient pressure values (HS $S = \frac{5}{2}$) down to about v=0.68. Further compression rapidly degrades the moment, which is accompanied by redistribution of electrons $e_g \rightarrow t_{2g}$ within the Mn $3d$ shell. The local moments and orbital occupancies start to level off to the LS values around $v = 0.57$. The reduction of M_{eff} below M_s in the LS state indicates that the local moment screening (charge fluctuations) is enhanced in comparison to the HS state.

Next we address the spectral properties. In Fig. 2 we compare the calculated total Mn $3d$ spectral function at ambient pressure with the photoemission data of van Elp *et al.* [20]. Excellent agreement is obtained for the gap and for the peak positions. (We note that using the enhanced J=1 eV gives significantly poorer agreement.) Having obtained a correct ambient pressure spectrum, we proceed in the study of the Mott transition by following the evolution with decreasing volume of the symmetry-resolved (t_{2g}, e_g) spectral densities, presented in Fig. 3. The onset of the moment collapse around $v = 0.68$ is signaled by, and associated with, closing of the gap in the t_{2g} channel, while the e_g gap is still easily visible at

$v = 0.63$. This orbital selectivity[21] in metalization cannot be an exact property since both e_g and t_{2g} bands hybridize with the same O $2p$ bands throughout the Brillouin zone; however, the smallness of t_{2g}–$2p$ mixing allows the orbital selectivity to be remarkably pronounced. As the t_{2g} gap closes, a quasiparticle peak appears at the chemical potential (E=0) as has been seen in simple models. Once in the LS state, the spectral functions bear strong resemblance to the parent LDA bands. In particular, the LDA ($U = J = 0$) t_{2g} spectrum contains a sharp peak just at/below the chemical potential, so it is not certain how much of the peak arising at the transition is due to the many-body nature of the system.

We now address a fundamental point of this work, namely the connection between moment collapse and metal-insulator transition, by observation of the impact of pressure on the effective Hamiltonian. Since U and J do not change, the pressure enters the calculation only through the quadratic part of the effective Hamiltonian. Reducing the role of pressure down to fundamentals one ends up with two effects: (i) broadening of the $3d$ bands and (ii) increase of the crystal-field splitting Δ_{cf}. (We define Δ_{cf} in terms of the site energies of the e_g and t_{2g} Wannier functions; the e_g–t_{2g} band splitting is substantially larger due to ligand field effects.) The evolution of the leading band structure quantities, which are the nearest-neighbor hopping amplitude $t_{pd\sigma}$, Δ_{cf}, and Δ_{ct} are shown in the inset of Fig. 5. Since the $3d$ bandwidth arises mainly through Mn $3d$ – O $2p$ hybridization ($W \propto t_{pd}^2/\Delta_{ct}$) the increase of t_{pd} hopping with pressure is to some extent compensated by the overall lowering of the p bands (increase in Δ_{ct}).

So far we have demonstrated a connection between the moment collapse and metal-insulator transition (MIT), yet the chicken-and-egg question – which property drives? which property follows? – is not yet answered. To this end we have performed an additional calculation at $v = 0.8$ (well within the insulating HS state) without *any* intra-atomic exchange (J=0). In spite of the large U and same U/W ratio, a LS solution is obtained, which is metallic although strongly renormalized. This result clearly shows that the MIT is *driven by the collapse of the moment*, which cannot withstand the increase of Δ_{cf}. The transition is characterized as evolving from five half-filled bands $t_{2g} + e_g$ (HS) to three t_{2g} bands with one hole per site (LS). The interaction energy cost of moving an electron from site to site is characterized by $U_{eff} = d^{n+1} + d^{n-1} - 2d^n$. Using the atomic configurations corresponding to HS and LS states one arrives at U_{eff} of 10.3 eV[18] and 5.9 eV respectively, indicating much

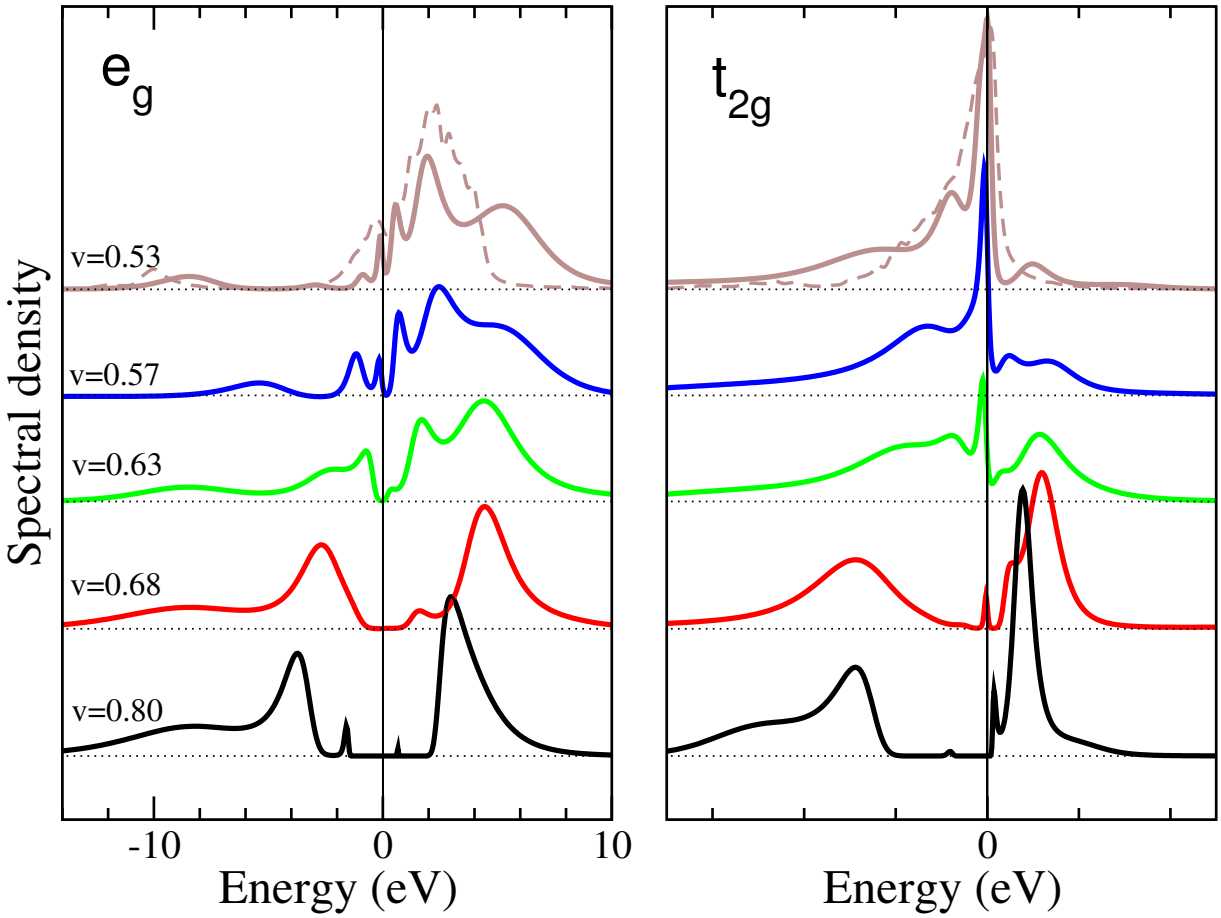

FIG. 3: The Mn-3d single-particle spectral functions resolved into e_g (left) and t_{2g} (right) irreducible representations for varying relative volume. Note the spectral weight shift under pressure: de-occupation of e_g occurs as the increase in occupation of t_{2g} proceeds (occupation $\equiv$ integrated weight over negative energies). For the lowest volume we show the uncorrelated (LDA) spectra for comparison (dotted lines). Apparently the main spectral features at high pressure originate from the uncorrelated band structure with some many-body renormalization. At even higher pressures the spectra remain qualitatively unchanged with some reduction of the weight of the high energy shoulders.

stronger inhibition of the electron propagation in HS state. Moreover, the Mn $3d(e_g)$ – O $2p$ hybridization provides an additional screening channel for the effective $t_{2g} - t_{2g}$ interaction in the LS state. Indeed, a calculation performed in the LS state with O $2p$ states integrated out (keeping the $3d$ bandwidth unchanged) before solving the interacting problem leads to more pronounced high energy shoulders as compared to the solution with O-p states fully

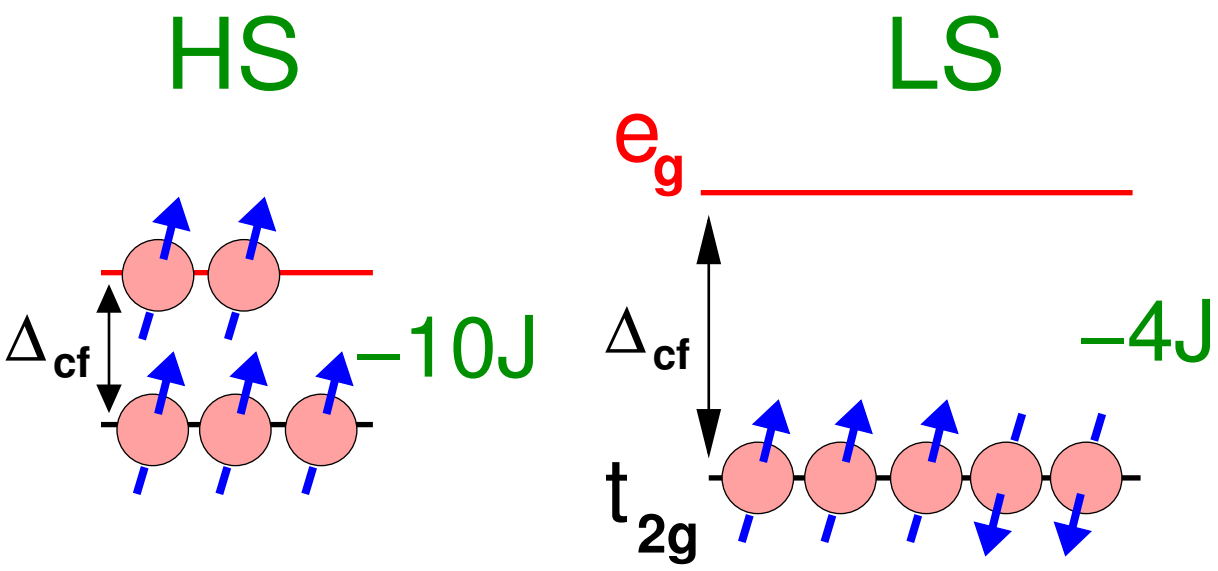

FIG. 4: Schematic energy diagrams of the high spin (left) and low spin (right) occupations of the Mn $3d$ levels. In the HS state two spin-up electrons occupy e_g orbitals at the cost of $2\Delta_{cf}$ in energy, but the spin-exchange energy gain is -$10J$ ($5\times4/2 = 10$ pairs of parallel spin electrons). In the LS state, the crystal field energy cost has become too great, and although the spin-exchange energy is less [-$4J$ from $3\times2/2$ (up) + 1 (down) = 4 pairs] there is a net energy gain. The LDA energy difference is also a factor.

included; an indication of stronger local correlations.

Our results establish that the transition is controlled by competition between the crystal-field spitting Δ_{cf} (favoring the LS state) and the intra-atomic exchange coupling J (favoring the HS state), of which only the former one is sensitive to an applied pressure. This sensitivity of results to the value of J was also found in LDA+U studies of the Mott transition.[13] Recently Werner and Millis [22] studied a two band model with competing intra-atomic exchange and crystal-field splitting. In the parameter range relevant for the present study they found three different phases realized in the following order with increasing crystal-field splitting: (i) spin-polarized Mott insulator, (ii) metal with large orbital and spin fluctuations and (iii) and orbitally polarized insulator. Moreover they found an orbitally selective closing of the gap upon doping in the vicinity to the (i)-(ii) phase boundary. The correspondence between the spin-polarized insulator (i) and the HS state of MnO is quite obvious. The transition region in MnO and phase (ii) are both characterized by metallization and strong

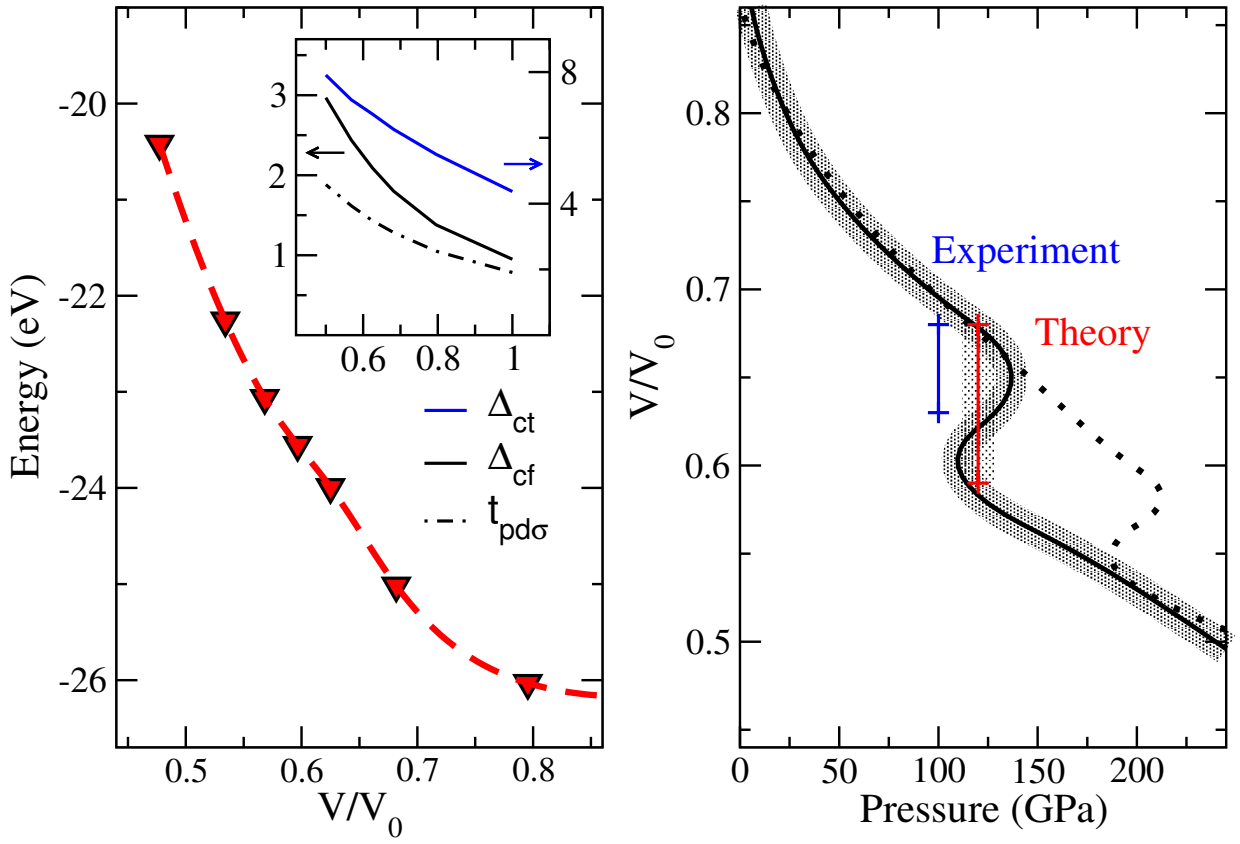

FIG. 5: The equation of state in two representations: internal energy versus volume (left panel), and volume versus pressure (right panel), obtained as a derivative of the spline interpolation of E(V). The red bar on the $V(P)$ curve lying at the theoretical transition pressure $P_c^{th} = 120 \pm 15$ GPa determines the volume collapse $v = 0.68 \rightarrow 0.59$. The dotted curve represents $V(P)$ for the enhanced value of exchange J=1 eV, showing the shift of the Mott transition to higher pressure with larger J. The error bar on P_c^{th} is estimated statistical uncertainty due to QMC statistical fluctuations. The inset in the left panel shows the evolution of selected tight-binding parameters (units of eV); note specifically the factor of three increase in Δ_{ct} .

orbital fluctuations as well as the orbitally selective gap behavior. Also the LS state of MnO and the phase (iii) of the model exhibit similarity, the orbital polarization. The insulating character of phase (iii) is dictated by band-filling and does not contradict the above analogy.

To compare to high pressure experiments, knowledge of phase stability is needed, which can be obtained from free energy vs volume (equation of state EOS). The theoretical justi-

fication for applying DMFT using the underlying LDA description relies on a well-defined thermodynamic grand canonical potential functional, for which specific realizations have been suggested.[23] Since it is difficult to extract the entropic term in the free energy we restrict ourselves to evaluation of the internal energy; in any case the variation of the entropy term is very small on the energy scale of several eV involved in the changes of total energy. We use the scheme of McMahan *et al.*[24] (which is similar to that of Savrasov and Kotliar[23]) corresponding to the expression $E(V,T) = E_{LDA}(V) + [E_{DMFT}(V,T) - E_{MF}(V)]$, where E_{LDA} is the all-electron (unpolarized) LDA energy, E_{DMFT} is the internal energy corresponding to the self-consistent (dynamic) DMFT solution for the effective Hamiltonian and E_{MF} is the static mean-field internal energy. The EOS curve is shown in Fig. 5. The main feature is the deviation from convexity in the transition region, which leads to a calculated volume collapse $v^{th} = 0.68 \rightarrow 0.59$ at $P_c^{th} = 120$ GPa. The metallization and moment collapse obtained here are not far from the high pressure data,[7–9] with the transition volume (pressure) being somewhat smaller (larger) than the experimental values $v_c^{exp} = 0.68 \rightarrow 0.63$, $P_c^{exp} = 100$ GPa.

These results demonstrate that the underlying LDA band structure, buttressed by on-site interactions (U, J) treated within the DMFT ansatz, provide a realistic description of the Mott transition in MnO without any input from experiment. This capability signals a quantum leap forward in our understanding of strongly correlated systems. This microscopic theory finally allows a determination of the mechanism of the transition, which could not be uncovered by experiment alone: the magnetic moment collapse, volume collapse, and metal-insulator transitions occur simultaneously, but it is the increasing crystal field splitting (encroachment of the O^{2-} ion on the internal structure of the Mn ion) and not the increasing bandwidth that tips the balance. This theory can now be applied to other Mott insulators to determine how generally this mechanism of metallization applies within the various oxide systems.

Acknowledgments: J.K. gratefully acknowledges the Research Fellowship of the Alexander von Humboldt Foundation. We acknowledge numerous discussions with D. Vollhardt and A. K. McMahan, and useful interaction with K.-W. Lee during the latter stages of this work. This work was supported by SFB 484 of the Deutsche Forschungsgemeinschaft (J.K.), by the Russian Foundation for Basic Research under the grants RFFI-06-02-81017, RFFI-07-

02-00041 (V.I.A. and A.V.L.) and the Dynasty Foundation (A.V.L.), and by DOE grant No. DE-FG02-04ER46111 and DOE's Computational Materials Science Network (J.K., R.T.S., and W.E.P.).

---

[1] Mott N. F. Proc. Phys. Soc. (London) **A62**, 416 (1949); Rev. Mod. Phys. **40**, 677 (1968).

[2] Imada M., Fujimori A., and Tokura Y. Rev. Mod. Phys. **70**, 1039 (1998).

[3] Saitoh T., Bouquet A. E., Mizokawa T., and Fujimori A., Phys. Rev. B **52**, 7934 (1995).

[4] Noguchi Y. *et al.*, Geophys. Res. Lett. **23**, 1469 (1996).

[5] Mita Y. *et al.*, Phys. Stat. Sol. (B) **223**, 247 (2001).

[6] Mita Y. *et al.* Phys. Rev. B **71**, 100101 (2005).

[7] Patterson J. R. *et al.*, Phys. Rev. B **69**, 220101 (2004).

[8] Yoo C. S. *et al.*, Phys. Rev. Lett. **94**, 115502 (2005).

[9] Rueff J.-P. *et al.*, J. Phys.: Cond. Matt. **17**, S717 (2005).

[10] Cohen R. E., Mazin I. I., and Isaak D. G., Science **275**, 654 (1997).

[11] Fang Z. *et al.*, Phys. Rev. B **59**, 762 (1999).

[12] Kasinathan D. *et al.*, Phys. Rev. B **74**, 195110 (2006).

[13] Kasinathan D., Koepernik K., and Pickett W. E., New J. Phys. **9**, 235 (2007).

[14] Held K. *et al.* phys. stat. solidi b **243**, 2599 (2006).

[15] Kuneš J., Anisimov V. I., Lukoyanov A. V., and Vollhardt D., Phys. Rev. B **75**, 165115 (2007); Kuneš J. *et al.*, arxiv/0705.1692.

[16] Georges A., Kotliar G., Krauth W., and Rozenberg M. J., Rev. Mod. Phys. **68**, 13 (1996); Kotliar G. and Vollhardt D., Phys. Today **57**(3), 53 (2004).

[17] Hirsch J. E. and Fye R. M., Phys. Rev. Lett. **56**, 2521 (1986).

[18] Anisimov V. I., Zaanen J., and Andersen O. K., Phys. Rev. B **44**, 943 (1991).

[19] Anisimov V. I. and Gunnarsson O., Phys. Rev. B **43**, 7570 (1991).

[20] van Elp J. *et al.*, Phys. Rev. B **44**, 1530 (1991).

[21] Liebsch A., Phys. Rev. Lett. **91**, 226401 (2003); Koga A. *et al.*, Phys. Rev. Lett. **92**, 216402 (2004).

[22] Werner P. and Millis A. J., arxiv/0704.0057.

[23] Savrasov S. Y. and Kotliar G., Phys. Rev. B **69**, 245101 (2004).

[24] McMahan A. K., Phys. Rev. B **72**, 115125 (2005); McMahan A. K., Held K., and Scalettar R. T., Phys. Rev. B **67**, 075108 (2003); *ibid.* **72**, 115125 (2005).